

Isospin mixing in a particle-number conserving microscopic approach

L. Bonneau¹, J. Bartel² and P. Quentin^{1,3}

¹*Theoretical Division, Los Alamos National Laboratory,
Los Alamos, NM 87545, USA*

²*Institut Pluridisciplinaire Hubert Curien,
CNRS/IN2P3 and Université Louis Pasteur 67000 Strasbourg, France*

³*Centre d'Etudes Nucléaires de Bordeaux-Gradignan,
Université Bordeaux-I and CNRS/IN2P3,
BP 120, 33175 Gradignan, France*

(Dated: November 15, 2018)

We calculate the isospin-mixing parameter for several $T_z = -1$, $T_z = 0$ and $T_z = 1$ nuclei from Mg to Sn in the particle-number conserving Higher Tamm–Dancoff approach taking into account the pairing correlations. In particular we investigate the role of the Coulomb interaction and the $|T_z| = 1$ pairing correlations. To do so the HTDA approach is implemented with the SIII Skyrme effective nucleon-nucleon interaction in the mean-field channel and a delta interaction in the pairing channel. We conclude from this investigation that the pairing correlations bring a large contribution to isospin-symmetry breaking, whereas the Coulomb interaction turns out to play a less important role. Moreover we find that the isospin-mixing parameters for $T_z = -1$ and $T_z = 1$ nuclei are comparable while they are about twice as large for $T_z = 0$ nuclei (between 3% and 6%, including doubly magic nuclei).

PACS numbers: 21.10.Hw, 21.60.Jz, 21.60.Cs

I. INTRODUCTION

One of the most striking aspect of the structure of atomic nuclei is the very small violation of the isobaric invariance. This is so even for heavy nuclei where the Coulomb interaction is not thought a priori to act merely in a perturbative manner. As pointed out for instance in Ref. [1], this is due to the weak variation of the symmetry-breaking Coulomb field over the nuclear volume. It has also been suggested from phenomenological and fundamental (at the levels of quarks having different masses) points of view that genuine isospin non-conserving parts of the strong interaction should be considered. They should however be rather small as compared to their conserving counterparts.

As a consequence, it has been found that a nuclear ground state $|\Psi\rangle$ may be thought as being composed of mostly a $T_0 = |T_z|$ component where $T_z = (N - Z)/2$ with a small $T_0 + 1$ admixture, namely

$$|\Psi\rangle \approx \beta|T_0 T_z\rangle + \alpha|T_0 + 1 T_z\rangle, \quad (1)$$

where $\alpha^2 + \beta^2 = 1$.

Even though in most cases the isobaric invariance may be flatly assumed, there are phenomena where a specific knowledge of the isospin mixing is needed. This is in particular the case whenever some observed transition or reaction would be forbidden, should this invariance be exactly fulfilled. Interesting cases, where the isospin mixing has to be considered, are also related with beta-decay properties (see, e.g., the review of Ref. [2]). Of particular importance in that respect are the studies of superallowed 0^+ -to- 0^+ nuclear β decays in the context of the tests of the CVC hypothesis (see, e.g., Ref. [3]) through ft -value measurements. Hence, a specific determination of the effect of the isospin mixing is required to correct the value yielded by the crude

isospin-multiplet approximation (determining thus the so-called δ_C corrective term).

Before entering, in a subsequent study, into a detailed assessment of the transition matrix element involved in such particular decays, we consider it interesting to evaluate first the actual importance of the isospin mixing as measured for instance by α^2 . This is the subject of the present paper.

Presently available theoretical estimates of the isospin mixing fall into three different categories.

First, one has to quote the hydrodynamical approach of Bohr, Damgård and Mottelson [4] which consists in quantifying the normal modes associated with the polarization effect of the Coulomb field on a spherically symmetrical isovector density. In $N = Z$ nuclei this approach yields the probability α^2 of the $T = 1$ component, in sole addition to the dominating $T = 0$ component, which is given by

$$\alpha^2 = 3.5 \times 10^{-7} Z^2 A^{2/3}. \quad (2)$$

It therefore amounts, e.g., for the ^{40}Ca nucleus to about 0.16%. In nuclei having a neutron excess, these authors estimate that α^2 (meaning now the probability of the $|T_z| + 1$ component over the dominating $|T_z|$ component) is equal to the value given by Eq. (2) divided by $|T_z| + 1$. This reduction, which is expressed in terms of a factor being merely the square of a Clebsch–Gordan coefficient, has been first advocated by Lane and Soper [5]. It yields, e.g., for the ^{48}Ca nucleus, a value of α^2 of about 0.04%.

The second class of approaches are based on shell-model calculations. Their success is contingent, as usual within such an approach, upon the relevance of the matrix elements in use. For the description of isospin mixing, an accurate determination of Coulomb matrix elements is of course of paramount importance (see for instance the discussion of Coulomb energy differences in $A = 47$ and $A = 49$ mirror pairs [6]). This constitutes an a priori necessary condition

to provide valuable answers to the question left open on the real importance of isospin non-conserving forces as studied for example to explain the isobaric multiplet yrast energies in Ref. [7]. Other concerns are related to a good description of radial single-particle wave functions as in, e.g., Ref. [8] to describe asymmetry factors in parity-violating electron scattering. One definite difficulty of shell-model calculations is due to the fact that they do not take into account any core isospin mixing, excepted of course for the no-core shell model calculations limited to very light nuclei (see for instance Ref. [9]).

One might then be inclined to think that microscopic calculations making use of phenomenological nucleon-nucleon forces should be able to describe the polarization effects of the Coulomb interaction at least at the mean field level, in a satisfactory way. Indeed, as opposed to shell-model calculations, mean-field calculations are expected to provide rather elaborate single-particle wave functions and they do not rely on any inert core approximation. However, apart from possible consequences of well-known symmetry violations inherent to the mean field approximation, they request as a next very important step to account accurately for the correlations. This may be done without serious a priori problems for RPA-type correlations, as performed for instance in [10, 11]. In Ref. [10], it is shown that the hydrodynamical ansatz of Ref. [4] underestimates the isospin mixing by a factor 2 to 4 (see Fig. 3 of [10]). It is important to note that the latter approach does not include important correlations, namely pairing correlations. There are good practical reasons for such an omission. The usual handling of pairing correlations within a kind of Bogoliubov quasiparticle vacuum approximation as in the BCS or Hartree–Fock–Bogoliubov theory is totally unfit for the isospin mixing problem. Indeed, such an ansatz yields spurious components of both charge state particle numbers, giving rise in turn to a spurious mixing of T_z -components which invalidates a priori any attempt to extract out of them any meaningful T -mixing properties.

This is why we make use here of the Higher Tamm–Dancoff approach (HTDA) which can be interpreted as a highly truncated shell model built on a self-consistent Hartree–Fock solution [12, 13, 14, 15]. At this stage we focus on the role of $|T_z| = 1$ pairing correlations, which gives us an upper limit of the isospin mixing parameter since proton-neutron pairing correlations are expected to reduce the isospin mixing as it will be discussed below. For the time-being we will not evaluate the effect of RPA correlations which could be (and will soon be) easily taken into account into the HTDA framework.

To determine α^2 , we should in principle perform a projection of the ground state $|\Psi\rangle$ on good isospin states $|T T_z\rangle$. Assuming, however, that components higher than T_0+1 are negligible, as in Eq. (1), we can deduce α^2 from the calculation of the expectation value of the square of the isospin operator \hat{T} in the state $|\Psi\rangle$. Indeed, if $|\Psi\rangle$ is normalized to unity and assuming that the dominant contribution of the

ground-state (GS) isospin comes from $T_0 = |T_z|$, we have

$$\langle\Psi|\hat{T}^2|\Psi\rangle = (1 - \alpha^2) T_0(T_0 + 1) + \alpha^2 (T_0 + 1)(T_0 + 2), \quad (3)$$

hence

$$\alpha^2 = \frac{\langle\Psi|\hat{T}^2|\Psi\rangle - T_0(T_0 + 1)}{2(T_0 + 1)}. \quad (4)$$

The paper is organized as follows. After the derivation of the expression for the expectation value of \hat{T}^2 in the state $|\Psi\rangle$ in Sect. II, we present in Sect. III the results of the HTDA calculations for the GS properties and the values of all relevant isospin quantities, such as the expectation value $\langle\Psi|\hat{T}^2|\Psi\rangle$, the deduced value of T and the isospin-mixing parameter α^2 for a large sample of nuclei. The main conclusions of this study are drawn in Sect. IV.

II. EXPECTATION VALUE OF \hat{T}^2 IN THE HIGHER TAMM–DANCOFF APPROACH

A. Correlated ground state in the Higher Tamm–Dancoff approach

Neglecting here the proton-neutron residual interaction, we can write the many-body state $|\Psi\rangle$ describing the ground state of a nucleus as the product of the correlated states $|\Psi^{(n)}\rangle$ and $|\Psi^{(p)}\rangle$

$$|\Psi\rangle = |\Psi^{(n)}\rangle \otimes |\Psi^{(p)}\rangle, \quad (5)$$

where, in the HTDA approach, $|\Psi^{(q)}\rangle$ ($q = n$ for neutrons and $q = p$ for protons) is a superposition of N_q -particle Slater determinants ($N_q = N$ for neutrons and $N_q = Z$ for protons) of the form

$$|\Psi^{(q)}\rangle = \chi_0^{(q)} |\Phi_0^{(q)}\rangle + \sum_{i>0} \chi_i^{(q)} |\Phi_i^{(q)}\rangle. \quad (6)$$

In Eq. (6), $|\Phi_0^{(q)}\rangle$ denotes the Hartree–Fock (HF) ground state and the $|\Phi_i^{(q)}\rangle$ are n -particle– n -hole excited states built on $|\Phi_0^{(q)}\rangle$ ¹. The a priori complex coefficients $\chi_0^{(q)}$ and $\chi_i^{(q)}$ are determined by minimizing the energy functional calculated for $|\Psi^{(q)}\rangle$. In fact, in order for the many-body state $|\Psi\rangle$, when constructed with real single particle wave functions, to be time-reversal invariant, the coefficients $\chi_0^{(q)}$ and $\chi_n^{(q)}$ must be real.

B. Expression of the expectation value of \hat{T}^2

Since \hat{T}^2 is an hermitian operator (see Appendix A for its definition and properties), its expectation value in the

¹ For the sake of clarity in the notation, we reserve the letter Φ for a Slater determinant and the letter Ψ for a correlated state.

HTDA state $|\Psi\rangle$ reads

$$\begin{aligned} \langle \Psi | \hat{\mathbf{T}}^2 | \Psi \rangle = & \sum_{i,j} (\chi_i^{(n)} \chi_j^{(p)})^2 (\langle \Phi_i^{(n)} | \otimes \langle \Phi_j^{(p)} |) \hat{\mathbf{T}}^2 (| \Phi_i^{(n)} \rangle \otimes | \Phi_j^{(p)} \rangle) \\ & + 2 \sum_{\substack{i \leq i', j \leq j' \\ (i', j') \neq (i, j)}} \chi_i^{(n)} \chi_j^{(p)} \chi_{i'}^{(n)} \chi_{j'}^{(p)} \times \\ & \text{Re} \left[(\langle \Phi_i^{(n)} | \otimes \langle \Phi_j^{(p)} |) \hat{\mathbf{T}}^2 (| \Phi_{i'}^{(n)} \rangle \otimes | \Phi_{j'}^{(p)} \rangle) \right], \end{aligned} \quad (7)$$

where $\text{Re}(z)$ denotes the real part of the complex number z . Since $\hat{\mathbf{T}}^2$ is a sum of one-body and two-body operators, the only contributions in the off-diagonal term of Eq.(7) are therefore those for which $|\Phi_i^{(n)}\rangle \otimes |\Phi_j^{(p)}\rangle$ and $|\Phi_{i'}^{(n)}\rangle \otimes |\Phi_{j'}^{(p)}\rangle$ differ by a particle-hole excitation of order less than or equal to 2. In the following it will be useful to recall that, if $|\Phi_i^{(n)}\rangle$ and $|\Phi_j^{(p)}\rangle$ are Slater determinants of N and Z particles, respectively, then $|\Phi_i^{(n)}\rangle \otimes |\Phi_j^{(p)}\rangle$ is a Slater determinant of $A = N + Z$ particles. Moreover, a Slater determinant $|\Phi_i\rangle$ without indication of its charge state q is to be understood as a product of a neutron $|\Phi_j^{(n)}\rangle$ and a proton $|\Phi_k^{(p)}\rangle$ Slater determinants. Finally we recall that the number of particles of each charge state q is even since we treat here even-even nuclei only.

Using the expressions for the isospin operator developed in Appendix A, it is easy to show that the diagonal matrix element of $\hat{\mathbf{T}}^2$ can be written in the form

$$\begin{aligned} (\langle \Phi_i^{(n)} | \otimes \langle \Phi_j^{(p)} |) \hat{\mathbf{T}}^2 (| \Phi_i^{(n)} \rangle \otimes | \Phi_j^{(p)} \rangle) = & \frac{A}{2} + \frac{(N-Z)^2}{4} \\ & - \sum_{k \in \Phi_i^{(n)}} \sum_{\ell \in \Phi_j^{(p)}} |\langle k | \ell \rangle_{\text{space-spin}}|^2, \end{aligned} \quad (8)$$

where the notations $\langle k | \ell \rangle_{\text{space-spin}}$ and $\sum_{k \in \Phi_i^{(n)}}$ are defined in Appendix A. It is important to note that the sums over the occupied single-particle states of $|\Phi_i^{(n)}\rangle$ and $|\Phi_j^{(p)}\rangle$ cannot be a priori reduced to sums over time-reversed partner states, except for the many-body states (including $|\Phi_0\rangle$) in which the single-particle states are all paired. When this is not the case, the contributions of the form $\langle \bar{k} | \ell \rangle_{\text{space-spin}}$ or $\langle k | \bar{\ell} \rangle_{\text{space-spin}}$ (where $|\bar{k}\rangle$ is the time-reversed partner of $|k\rangle$) vanish. Therefore the expectation value of $\hat{\mathbf{T}}^2$ in the Hartree-Fock ground state $|\Phi_0\rangle$ is a special case of Eq. (8).

The contribution $\langle \Psi | \hat{\mathbf{T}}^2 | \Psi \rangle_{\text{diag}}$ of the diagonal terms in Eq. (8) to the expectation value of $\hat{\mathbf{T}}^2$ finally writes

$$\begin{aligned} \langle \Psi | \hat{\mathbf{T}}^2 | \Psi \rangle_{\text{diag}} = & \frac{A}{2} + \frac{(N-Z)^2}{4} \\ & - \sum_{i,j} (\chi_i^{(n)} \chi_j^{(p)})^2 \sum_{k \in \Phi_i^{(n)}} \sum_{\ell \in \Phi_j^{(p)}} |\langle k | \ell \rangle_{\text{space-spin}}|^2. \end{aligned} \quad (9)$$

To calculate the off-diagonal matrix elements we can exploit the fact that one of the two Slater determinants of a given charge state is expressed as a n -particle- n -hole excitation with respect to the other one. This gives simple expressions for the matrix elements but for each pair of Slater determinants $|\Phi_i^{(q)}\rangle$ and $|\Phi_j^{(q)}\rangle$ we have to determine the single-particle states $|i_1\rangle, \dots, |i_n\rangle, |j_1\rangle, \dots, |j_n\rangle$ (hole or particle states of $|\Phi_0\rangle$) such that $|\Phi_j^{(q)}\rangle = \varphi_{ij} a_{i_1}^\dagger \dots a_{i_n}^\dagger a_{j_1} \dots a_{j_n} |\Phi_i^{(q)}\rangle$, where $\varphi_{ij} = \pm 1$ is a phase factor determined in Appendix B.

The non vanishing off-diagonal matrix element of $\hat{\mathbf{T}}^2$ involving two Slater determinants differing by a 1-particle-1-hole excitation $a_i^\dagger a_j$ with $i \neq j$ is given by

$$\begin{aligned} (\langle \Phi_i^{(n)} | \otimes \langle \Phi_j^{(p)} |) \hat{\mathbf{T}}^2 a_k^\dagger a_\ell (| \Phi_i^{(n)} \rangle \otimes | \Phi_j^{(p)} \rangle) = & \\ & - \delta_{kn} \delta_{\ell n} \sum_{m \in \Phi_j^{(p)}} \langle \ell | m \rangle_{\text{space-spin}} \langle m | k \rangle_{\text{space-spin}} \\ & - \delta_{kp} \delta_{\ell p} \sum_{m \in \Phi_i^{(n)}} \langle \ell | m \rangle_{\text{space-spin}} \langle m | k \rangle_{\text{space-spin}}. \end{aligned} \quad (10)$$

Finally, for two Slater determinants differing by a 2-particle-2-hole excitation $a_{i_1}^\dagger a_{i_2}^\dagger a_{j_1} a_{j_2}$ with $\{i_1, i_2\} \cap \{j_1, j_2\} = \emptyset$, we have

$$\begin{aligned} (\langle \Phi_i^{(n)} | \otimes \langle \Phi_j^{(p)} |) \hat{\mathbf{T}}^2 a_{k_1}^\dagger a_{k_2}^\dagger a_{\ell_1} a_{\ell_2} (| \Phi_i^{(n)} \rangle \otimes | \Phi_j^{(p)} \rangle) = & \\ (\delta_{k_1 n} \delta_{k_2 p} \delta_{\ell_1 p} \delta_{\ell_2 n} + \delta_{k_1 p} \delta_{k_2 n} \delta_{\ell_1 n} \delta_{\ell_2 p}) \times & \\ \langle \ell_1 | k_1 \rangle_{\text{space-spin}} \langle \ell_2 | k_2 \rangle_{\text{space-spin}} & \\ - (\delta_{k_1 p} \delta_{k_2 n} \delta_{\ell_1 p} \delta_{\ell_2 n} + \delta_{k_1 n} \delta_{k_2 p} \delta_{\ell_1 n} \delta_{\ell_2 p}) \times & \\ \langle \ell_1 | k_2 \rangle_{\text{space-spin}} \langle \ell_2 | k_1 \rangle_{\text{space-spin}}. & \end{aligned} \quad (11)$$

From Eqs. (10) and (11) we deduce that the non vanishing off-diagonal contribution $\langle \Psi | \hat{\mathbf{T}}^2 | \Psi \rangle_{\text{off-diag}}$ to the expectation value of $\hat{\mathbf{T}}^2$ takes the form

$$\begin{aligned} \langle \Psi | \hat{\mathbf{T}}^2 | \Psi \rangle_{\text{off-diag}} = & 2 \sum_{i,j} \chi_i^{(n)} (\chi_j^{(p)})^2 \sum_{i'=1\text{p1h}(i)} \chi_{i'}^{(n)} (\langle \Phi_i^{(n)} | \otimes \langle \Phi_j^{(p)} |) \hat{\mathbf{T}}^2 (| \Phi_{i'}^{(n)} \rangle \otimes | \Phi_j^{(p)} \rangle) \\ & + 2 \sum_{i,j} (\chi_i^{(n)})^2 \chi_j^{(p)} \sum_{j'=1\text{p1h}(j)} \chi_{j'}^{(p)} (\langle \Phi_i^{(n)} | \otimes \langle \Phi_j^{(p)} |) \hat{\mathbf{T}}^2 (| \Phi_i^{(n)} \rangle \otimes | \Phi_{j'}^{(p)} \rangle) \\ & + 2 \sum_{i,j} \chi_i^{(n)} \chi_j^{(p)} \sum_{\substack{i'=1\text{p1h}(i) \\ j'=1\text{p1h}(j)}} \chi_{i'}^{(n)} \chi_{j'}^{(p)} (\langle \Phi_i^{(n)} | \otimes \langle \Phi_j^{(p)} |) \hat{\mathbf{T}}^2 (| \Phi_{i'}^{(n)} \rangle \otimes | \Phi_{j'}^{(p)} \rangle). \end{aligned} \quad (12)$$

The first two terms of $\langle \Psi | \hat{\mathbf{T}}^2 | \Psi \rangle_{\text{off-diag}}$ are calculated using respectively the first or the second term of the right hand side of Eq. (10), whereas the third term of $\langle \Psi | \hat{\mathbf{T}}^2 | \Psi \rangle_{\text{off-diag}}$ corresponds to one of the four series of δ products in the right hand side of Eq. (11). In practice, the sum of all off-diagonal terms is at least two orders of magnitude smaller than $\langle \Psi | \hat{\mathbf{T}}^2 | \Psi \rangle_{\text{diag}}$.

C. Limiting cases

We consider in this subsection two relevant limiting cases: the Hartree–Fock limit and the limit of identical neutron and proton single-particle states. We will refer to these limits in Sect. III to interpret some results.

In the Hartree–Fock limit where $\chi_i^{(\tau)} = \delta_{i0}$, we can deduce from Eqs. (8), (10) and (11) that the off-diagonal matrix elements vanish. The expectation value of $\hat{\mathbf{T}}^2$ thus simply becomes

$$\langle \Psi | \hat{\mathbf{T}}^2 | \Psi \rangle = \langle \Phi_0 | \hat{\mathbf{T}}^2 | \Phi_0 \rangle = \frac{A}{2} + \frac{(N-Z)^2}{4} - \sum_{k \in \Phi_0^{(n)}} \sum_{\ell \in \Phi_0^{(p)}} |\langle k | \ell \rangle_{\text{space-spin}}|^2. \quad (13)$$

In the limit where the neutron and proton single-particle states are assumed to be identical, the diagonal contribution (9) to $\langle \Psi | \hat{\mathbf{T}}^2 | \Psi \rangle$ becomes

$$\langle \Psi | \hat{\mathbf{T}}^2 | \Psi \rangle_{\text{diag}} = T_0(T_0 + 1) + \sum_{\substack{i,j \\ (i,j) \neq (0,0)}} (\chi_i^{(n)} \chi_j^{(p)})^2 \mathcal{R}(\Phi_i^{(n)}, \Phi_j^{(p)}), \quad (14)$$

where $T_0 = |T_z|$ and $\mathcal{R}(\Phi_i^{(n)}, \Phi_j^{(p)})$ denotes the relative excitation order of $|\Phi_i^{(n)}\rangle$ with respect of $|\Phi_j^{(p)}\rangle$ (see Eq. (B-8) of Appendix B). Therefore the isospin-mixing parameter takes, in this model case of identical neutron and proton single-particle states, the simple form

$$\alpha^2 = \frac{1}{2(T_0 + 1)} \sum_{\substack{i,j \\ (i,j) \neq (0,0)}} (\chi_i^{(n)} \chi_j^{(p)})^2 \mathcal{R}(\Phi_i^{(n)}, \Phi_j^{(p)}). \quad (15)$$

III. RESULTS AND DISCUSSION

We study the isospin symmetry breaking through the isospin-mixing parameter α^2 defined in Eq. (4) for $T_z = -1$, $T_z = 0$ and $T_z = 1$ nuclei of eight elements, namely $Z = 12$ (Mg), $Z = 16$ (S), $Z = 20$ (Ca), $Z = 24$ (Cr), $Z = 28$ (Ni), $Z = 36$ (Kr), $Z = 40$ (Zr) and $Z = 50$ (Sn).

To evaluate the expectation value $\langle \Psi | \hat{\mathbf{T}}^2 | \Psi \rangle$ we need a reliable description of the ground states of these nuclei. For that purpose, we follow the two-step approach of Ref. [15] where it was applied to study GS pairing properties of $N = Z$ nuclei in the mass $A \approx 70$ region. Since the above considered nuclei exhibit no triaxial deformation in their

ground state, we can search for GS solutions possessing axial symmetry. In the first step, we determine the GS deformation within the Hartree–Fock–BCS (HFBCS) approach. To do so, we use the Skyrme interaction in its SIII parametrization [16] in the mean-field channel, and the seniority force in the pairing channel. For the latter we retain the same set of parameters as in Ref. [15], where they were adjusted to reproduce experimental odd-even mass differences through a 3-point formula ($G_0^{(n)} = 17.70$ MeV, $G_0^{(p)} = 15.93$ MeV, $\Delta\epsilon = 6$ MeV and $\mu = 0.2$ MeV). In practice, we use 15 oscillator major shells to expand the single-particle states on the cylindrical harmonic-oscillator basis and optimize the basis parameters at the GS deformation so as to obtain the lowest HFBCS binding energy. In the second step, we calculate GS properties in the HTDA approach from the above HFBCS solution. The residual interaction employed is the delta interaction of Ref. [15] adjusted in the same way as above for the seniority force but with $\Delta\epsilon = 12$ MeV. The optimal values $V_0^{(q)}$ of the strength were found to be $V_0^{(n)} = -340$ MeV.fm³ and $V_0^{(p)} = -306$ MeV.fm³ (this fit has been performed on the neutron pairing strength upon the simple approximation that $V_0^{(p)}$ is quenched by 10% with respect to $V_0^{(n)}$ because of the anti-pairing contribution of the Coulomb interaction). However, keeping the same interaction strength throughout the whole considered nuclear region, we have taken care of the well-known $A^{-1/3}$ energy scale by varying the active pairing window: $\Delta\epsilon = 12 \times (72/A)^{1/3}$ MeV and $\mu = 0.2 \times (72/A)^{1/3}$ MeV, which yields for $A = 72$ the same window parameters as those of Ref. [15].

The GS properties calculated here are the charge radius r_c , the β_2 deformation parameter (see Appendix C), the mass quadrupole (Q_{20}) and hexadecapole (Q_{40}) moments, the neutron and proton pair-condensation energies $E_{\text{cond}}^{(q)}$, the trace of the operator $\sqrt{\hat{\rho}(1-\hat{\rho})}$, which is equal to the sum $\sum_i u_i v_i$ with $u_i = \sqrt{1-v_i^2}$ and $v_i = \sqrt{\rho_{ii}}$, with $\hat{\rho}$ being the one-body density (see Ref. [15]), and the total binding energy E_b . The results are reported in Table I.

The resulting HTDA ground state $|\Psi\rangle$ is then used to calculate the expectation value of the $\hat{\mathbf{T}}^2$ operator. In practice the off-diagonal term (12) turns out to be negligible with respect to the diagonal contribution (9) and therefore can be safely omitted in the calculations. Then, from the value of $\langle \Psi | \hat{\mathbf{T}}^2 | \Psi \rangle$, we deduce the T -value defined by

$$\langle \Psi | \hat{\mathbf{T}}^2 | \Psi \rangle = T(T + 1). \quad (16)$$

We present the values of $\langle \Psi | \hat{\mathbf{T}}^2 | \Psi \rangle$, T and α^2 in the columns labeled ‘‘HTDA’’ in Table II and in Fig. 1 we show the variation with Z of the isospin-mixing parameter α^2 within the HTDA approach for the above twenty four nuclei. Apart from a dip around ^{56}Ni , α^2 increases with Z , faster for the $N = Z$ nuclei than for the others. Moreover the dip is deeper for the former nuclei. We also note that the isospin-mixing parameters for $T_z = -1$ and $T_z = 1$ nuclei are very similar and are about a factor of two smaller than for $T_z = 0$ nuclei.

A precise determination of the isospin-mixing parameter

TABLE I: Ground-state properties of the twenty-one studied nuclei calculated within the HTDA approach. from left to right: the charge radius r_c , the β_2 deformation parameter (calculated as in Eq. (C-6) of Appendix C), the mass quadrupole (Q_{20}) and hexadecapole (Q_{40}) moments, the neutron and proton pair-condensation energies $E_{\text{cond}}^{(q)}$.

Nucleus	r_c (fm)	β_2	Q_{20} (fm ²)	Q_{40} (fm ⁴)	E_{cond} (MeV)		$\sum_i u_i v_i$		E_b (MeV)
					n	p	n	p	
²² Mg	3.107	0.346	92.1	147.8	-0.737	-0.687	1.391	1.408	-169.038
²⁴ Mg	3.127	0.362	110.2	105.4	-0.669	-0.542	1.232	1.133	-196.350
²⁶ Mg	3.085	0.220	69.4	42.4	-0.715	-0.574	1.445	1.337	-215.591
³⁰ S	3.262	0.000	-0.0	0.1	-0.562	-0.521	1.191	1.385	-242.770
³² S	3.299	0.192	83.3	-35.2	-0.604	-0.488	1.299	1.184	-268.322
³⁴ S	3.309	0.096	44.3	-8.8	-0.838	-0.501	2.027	1.352	-287.737
³⁸ Ca	3.479	-0.002	-1.0	-0.0	-0.855	-0.774	3.206	1.662	-311.842
⁴⁰ Ca	3.497	0.000	0.0	0.0	-0.727	-0.656	1.488	1.516	-342.405
⁴² Ca	3.510	-0.003	-1.6	1.8	-1.578	-0.530	4.525	1.284	-361.798
⁴⁶ Cr	3.666	0.158	120.9	356.1	-0.837	-0.769	2.242	2.087	-380.765
⁴⁸ Cr	3.709	0.241	203.7	666.9	-0.670	-0.571	1.632	1.524	-409.845
⁵⁰ Cr	3.708	0.210	185.2	326.3	-0.692	-0.557	1.714	1.581	-434.312
⁵⁴ Ni	3.788	0.002	2.0	-0.4	-1.058	-0.393	4.259	1.201	-452.236
⁵⁶ Ni	3.803	0.000	-0.0	0.1	-0.442	-0.362	1.254	1.148	-483.833
⁵⁸ Ni	3.828	0.002	2.3	-0.3	-0.652	-0.353	3.378	1.137	-502.966
⁷⁰ Kr	4.193	-0.308	-395.4	799.7	-0.536	-0.572	1.701	1.863	-573.651
⁷² Kr	4.222	-0.352	-468.1	1140.3	-0.531	-0.479	1.670	1.647	-601.580
⁷⁴ Kr	4.235	-0.350	-487.0	1092.7	-0.724	-0.443	2.658	1.581	-624.463
⁷⁸ Zr	4.392	0.392	785.9	1901.3	-0.485	-0.450	1.594	1.614	-636.298
⁸⁰ Zr	4.414	0.398	834.2	1589.4	-0.503	-0.456	1.663	1.606	-663.977
⁸² Zr	4.439	0.418	919.0	2221.2	-0.486	-0.445	1.753	1.586	-687.473
⁹⁸ Sn	4.524	0.000	-0.7	-10.6	-0.841	-0.367	4.992	1.430	-793.287
¹⁰⁰ Sn	4.535	0.000	0.1	-0.1	-0.418	-0.349	1.498	1.392	-826.870
¹⁰² Sn	4.554	0.000	-0.1	7.6	-0.709	-0.342	5.277	1.381	-846.359

requires that some great care be exerted in the calculations. This is illustrated in some typical examples in Appendix D. Here we merely discuss the most important points.

First of all, we need to make sure that we have obtained a perfect consistency between the wave functions and the mean field including its Coulomb isospin-breaking part. In Appendix D we show that a poor convergence of the iterative process may lead to drastic distortions in the isospin mixing evaluations.

A second important point is related to the quantal character of the assessed quantity. As exemplified in Appendix D, it appears that in order to get reliable α^2 values, one should include almost all Slater determinant components $|\Phi_i\rangle$ of the correlated wave function $|\Psi\rangle$, even those appearing in $|\Psi\rangle$ with a relatively minute probability $(\chi_i^{(q)})^2$, because of constructive interference effects.

A last technical point is worth noting here. It deals with the question of the independence of our results with the harmonic oscillator basis parameters b and q (see their definition, e.g., in Ref. [17]) in the expansion of the single-

particle wave functions. One might have been concerned by the fact that this optimization has been performed merely at the level of the preliminary HFBCS calculations and not at the final stage of our HTDA approach. However it has been checked that an energy optimization of HTDA results leaves unchanged the calculated α^2 values, as shown on one example in Appendix D.

We now investigate several sources of isospin symmetry breaking.

A. Roles of the neutron-proton mass difference and the Coulomb interaction

We investigate separately the sensitivity of our results to the neutron-proton mass difference and to the presence of the Coulomb interaction.

It turns out that the former plays virtually no role at all. For ⁴⁰Ca, for instance, upon suppressing the one-body center of mass correction (involving a $1/A$ term, ambiguous in this context), we found that the mass difference is

TABLE II: Expectation value of \hat{T}^2 , isospin T from Eq. (16) and isospin-mixing parameter α^2 from Eq. (4) calculated within the HTDA and HFBCS approaches at the ground states determined in Table I. The columns labeled “HF” correspond to the contributions to the above three quantities coming from the Slater determinant $|\Phi_0\rangle$ in the HTDA ground state expansion of Eqs. (5) and (6). The values given in italic are obtained without Coulomb interaction.

Nucleus	$\langle\Psi \hat{T}^2 \Psi\rangle$			T			α^2 (%)			
	HTDA	“HF”	HFBCS	HTDA	“HF”	HFBCS	HTDA	“HF”	HFBCS	
$T_z = -1$	^{22}Mg	2.054	2.018	2.137	1.018	1.006	1.045	1.3	0.5	3.4
		<i>2.049</i>	<i>2.014</i>	<i>2.186</i>	<i>1.016</i>	<i>1.005</i>	<i>1.061</i>	<i>1.2</i>	<i>0.3</i>	<i>4.6</i>
	^{30}S	2.046	2.009	2.362	1.015	1.003	1.116	1.2	0.2	9.1
		<i>2.038</i>	<i>2.003</i>	<i>2.270</i>	<i>1.013</i>	<i>1.001</i>	<i>1.088</i>	<i>0.9</i>	<i>0.1</i>	<i>6.8</i>
	^{38}Ca	2.077	2.025	2.904	1.025	1.008	1.276	1.9	0.6	22.6
		<i>2.052</i>	<i>2.003</i>	<i>2.890</i>	<i>1.017</i>	<i>1.001</i>	<i>1.272</i>	<i>1.3</i>	<i>0.1</i>	<i>22.3</i>
	^{46}Cr	2.090	2.016	3.769	1.030	1.005	1.505	2.3	0.4	44.2
	^{54}Ni	2.048	2.019	2.857	1.016	1.006	1.263	1.2	0.5	21.4
		<i>2.030</i>	<i>2.003</i>	<i>2.837</i>	<i>1.010</i>	<i>1.001</i>	<i>1.257</i>	<i>0.8</i>	<i>0.1</i>	<i>20.9</i>
	^{70}Kr	2.091	2.038	3.967	1.030	1.013	1.554	2.3	1.0	49.2
<i>2.054</i>		<i>2.003</i>	<i>4.398</i>	<i>1.018</i>	<i>1.001</i>	<i>1.656</i>	<i>1.3</i>	<i>0.1</i>	<i>60.0</i>	
^{78}Zr	2.085	2.043	2.680	1.028	1.014	1.212	2.1	1.1	17.0	
	<i>2.043</i>	<i>2.005</i>	<i>2.772</i>	<i>1.014</i>	<i>1.002</i>	<i>1.238</i>	<i>1.1</i>	<i>0.1</i>	<i>19.3</i>	
^{98}Sn	2.093	2.068	2.896	1.031	1.022	1.274	2.3	1.7	22.4	
	<i>2.024</i>	<i>2.002</i>	<i>2.832</i>	<i>1.008</i>	<i>1.001</i>	<i>1.256</i>	<i>0.6</i>	<i>0.0</i>	<i>20.8</i>	
$T_z = 0$	^{24}Mg	0.060	0.003	0.003	0.057	0.003	0.003	3.0	0.2	0.2
		<i>0.056</i>	<i>0.000</i>	<i>0.000</i>	<i>0.054</i>	<i>0.000</i>	<i>0.000</i>	<i>2.8</i>	<i>0.0</i>	<i>0.0</i>
	^{32}S	0.066	0.008	0.008	0.062	0.007	0.007	3.3	0.4	0.4
		<i>0.057</i>	<i>0.000</i>	<i>0.000</i>	<i>0.054</i>	<i>0.000</i>	<i>0.000</i>	<i>2.8</i>	<i>0.0</i>	<i>0.0</i>
	^{40}Ca	0.085	0.011	0.011	0.078	0.011	0.011	4.2	0.5	0.5
		<i>0.070</i>	<i>0.000</i>	<i>0.000</i>	<i>0.066</i>	<i>0.000</i>	<i>0.000</i>	<i>3.5</i>	<i>0.0</i>	<i>0.0</i>
	^{48}Cr	0.092	0.015	0.163	0.085	0.015	0.142	4.6	0.8	8.1
		<i>0.081</i>	<i>0.000</i>	<i>0.545</i>	<i>0.076</i>	<i>0.000</i>	<i>0.392</i>	<i>4.1</i>	<i>0.0</i>	<i>27.3</i>
	^{56}Ni	0.062	0.020	0.020	0.059	0.020	0.020	3.1	1.0	1.0
		<i>0.040</i>	<i>0.000</i>	<i>0.000</i>	<i>0.038</i>	<i>0.000</i>	<i>0.000</i>	<i>2.0</i>	<i>0.0</i>	<i>0.0</i>
^{72}Kr	0.107	0.038	0.978	0.098	0.037	0.608	5.4	1.9	48.9	
	<i>0.068</i>	<i>0.000</i>	<i>1.667</i>	<i>0.064</i>	<i>0.000</i>	<i>0.885</i>	<i>3.4</i>	<i>0.0</i>	<i>83.4</i>	
^{80}Zr	0.105	0.046	1.083	0.096	0.044	0.655	5.2	2.3	54.2	
	<i>0.051</i>	<i>0.000</i>	<i>1.091</i>	<i>0.049</i>	<i>0.000</i>	<i>0.658</i>	<i>2.6</i>	<i>0.0</i>	<i>54.6</i>	
^{100}Sn	0.113	0.073	0.073	0.103	0.069	0.069	5.7	3.7	3.7	
	<i>0.036</i>	<i>0.000</i>	<i>0.000</i>	<i>0.035</i>	<i>0.000</i>	<i>0.000</i>	<i>1.8</i>	<i>0.0</i>	<i>0.0</i>	
$T_z = 1$	^{26}Mg	2.062	2.025	2.189	1.020	1.008	1.062	1.5	0.6	4.7
		<i>2.057</i>	<i>2.021</i>	<i>2.269</i>	<i>1.019</i>	<i>1.007</i>	<i>1.087</i>	<i>1.4</i>	<i>0.5</i>	<i>6.7</i>
	^{34}S	2.057	2.003	3.493	1.019	1.001	1.435	1.4	0.1	37.3
		<i>2.055</i>	<i>2.003</i>	<i>3.362</i>	<i>1.018</i>	<i>1.001</i>	<i>1.401</i>	<i>1.4</i>	<i>0.1</i>	<i>34.0</i>
	^{42}Ca	2.056	2.018	3.037	1.018	1.006	1.313	1.4	0.4	25.9
		<i>2.041</i>	<i>2.004</i>	<i>3.029</i>	<i>1.013</i>	<i>1.001</i>	<i>1.311</i>	<i>1.0</i>	<i>0.1</i>	<i>25.7</i>
	^{50}Cr	2.072	2.026	2.528	1.024	1.009	1.167	1.8	0.7	13.2
		<i>2.052</i>	<i>2.008</i>	<i>2.726</i>	<i>1.017</i>	<i>1.003</i>	<i>1.225</i>	<i>1.3</i>	<i>0.2</i>	<i>18.2</i>
	^{58}Ni	2.049	2.018	3.193	1.016	1.006	1.356	1.2	0.5	29.8
		<i>2.030</i>	<i>2.001</i>	<i>3.129</i>	<i>1.010</i>	<i>1.000</i>	<i>1.338</i>	<i>0.8</i>	<i>0.0</i>	<i>28.2</i>
^{74}Kr	2.094	2.042	3.910	1.031	1.014	1.540	2.3	1.1	47.7	
^{82}Zr	2.090	2.044	3.624	1.030	1.015	1.468	2.3	1.1	40.6	
^{102}Sn	2.094	2.069	3.582	1.031	1.023	1.458	2.3	1.7	39.5	
	<i>2.022</i>	<i>2.000</i>	<i>3.437</i>	<i>1.007</i>	<i>1.000</i>	<i>1.420</i>	<i>0.6</i>	<i>0.0</i>	<i>35.9</i>	

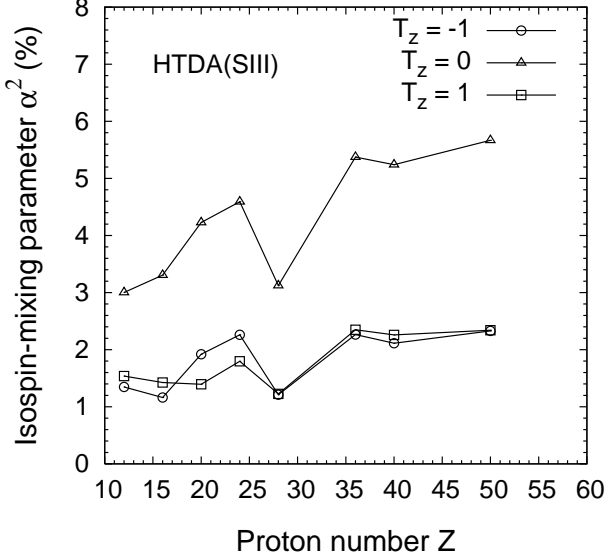


FIG. 1: Variation with Z of the isospin-mixing parameter α^2 calculated within the HTDA approach for $T_z = -1$ (open circles), $T_z = 0$ (open triangles) and $T_z = 1$ (open squares) nuclei.

responsible for a variation in α^2 of the order of one part in 10^4 . It is neglected in the remainder of the paper.

As can be seen from the columns “HTDA” of Table II where the results obtained without the Coulomb interaction are shown in *italic*, the Coulomb interaction has a more noticeable effect which still remains rather weak for the light nuclei considered here. In this comparative study, we do not include the results for ^{46}Cr , ^{74}Kr and ^{82}Zr because the GS solutions without Coulomb interaction differ too much from the ones obtained in the full calculations to make a comparison meaningful.

B. Role of the particle-number conservation

A very interesting issue consists in investigating the quality of the particle-number conserving pairing treatment (here in the $|T_z| = 1$ channel only) obtained by the HTDA approach as compared to approximations (as in the HFBCS calculations preliminary to our HTDA evaluation) which violate particle-number conservation. For that purpose, we evaluate the expectation value of $\hat{\mathbf{T}}^2$ from the HFBCS ground state and deduce the value of the isospin-mixing parameter through Eq. (4). The expectation value of $\hat{\mathbf{T}}^2$ in a BCS state normalized to unity, noted $|\text{BCS}\rangle$, reads

$$\begin{aligned} \langle \text{BCS} | \hat{\mathbf{T}}^2 | \text{BCS} \rangle &= A + \frac{1}{4} (N - Z)^2 - \sum_{i>0} v_i^4 \\ &- 2 \sum_{i>0}^{(n)} v_i^2 \sum_{k>0}^{(p)} v_k^2 |\langle i | k \rangle_{\text{space-spin}}|^2, \end{aligned} \quad (17)$$

where the sums $\sum_{i>0}^{(n)}$, $\sum_{k>0}^{(p)}$ and $\sum_{i>0}$ run over neutron, proton and all pairs of time-reversed single-particle

states of the form $\{|i\rangle, |\bar{i}\rangle\}$, respectively. The resulting values of $\langle \text{BCS} | \hat{\mathbf{T}}^2 | \text{BCS} \rangle$, T and α^2 are reported in the columns labeled “BCS” of Table II.

In cases where pairing correlations are ineffective in the BCS treatment (one is then below the phase transition to the superfluid phase), the value of α^2 is very small, since in that case essentially a single Slater determinant is describing the nuclear state and the particle number is trivially conserved. In contrast, for those nuclei where pairing plays a non negligible role, the values of the parameter α^2 turn out to take on completely unrealistic values as, e.g., for the nuclei ^{38}Ca or ^{80}Zr . In fact, as shown in Fig. 2, there is a strong correlation between α^2 calculated in the HFBCS approach and the particle-number fluctuation $\Delta N + \Delta Z$ in the BCS state, where ΔN_q is defined by

$$\Delta N_q = \sqrt{\langle \text{BCS} | \hat{N}_q^2 | \text{BCS} \rangle - N_q^2}. \quad (18)$$

With the exception of ^{72}Kr and ^{80}Zr , all the points lie approximately on a straight line in the $(\alpha^2, \Delta N + \Delta Z)$ plane as can be seen in Fig. 2.

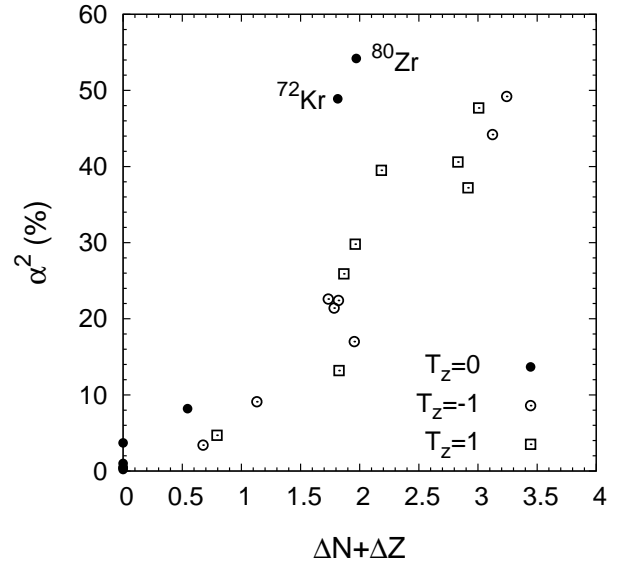


FIG. 2: Correlation between α^2 and the particle-number fluctuation $\Delta N + \Delta Z$ within the HFBCS approach for all twenty four $T_z = -1$, $T_z = 0$ and $T_z = 1$ nuclei.

C. Role of the pairing correlations

In order to assess the importance of pairing correlations on the isospin-mixing rate, we also calculate the expectation value of $\hat{\mathbf{T}}^2$ in the Slater determinant $|\Phi_0\rangle$ using Eq. (13). The resulting values for $\langle \Phi_0 | \hat{\mathbf{T}}^2 | \Phi_0 \rangle$, T and α^2 are reported in the columns labeled “HF” of Table II. In general $\langle \Phi_0 | \hat{\mathbf{T}}^2 | \Phi_0 \rangle$ is different from the value that would result from a pure HF calculation because $|\Phi_0\rangle$ is the Slater determinant built up from the single-particle states resulting from the first-step HFBCS calculation. This difference

vanishes of course for nuclei in which BCS predicts no pairing correlations, which is the case here for the doubly magic nuclei as well as ^{24}Mg and ^{32}S .

For nuclei exhibiting weak pairing correlations, the ‘‘HF’’ results are, quite expectedly, close to the HTDA predictions. Otherwise, the HTDA results are significantly larger than the ‘‘HF’’ ones. The $T_z = 0$ pairing correlations are therefore an important source of isospin symmetry breaking. This is conspicuous from Fig. 3 which shows the strong correlation between the variations of α^2 and $\sum_i u_i v_i$ with Z for $N = Z$ nuclei.

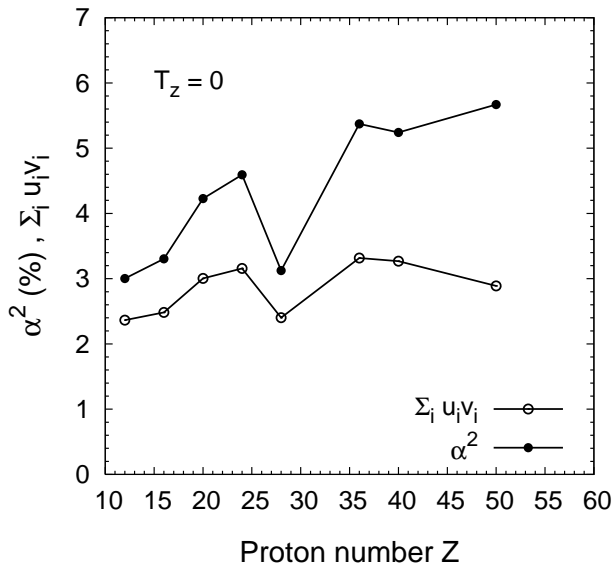


FIG. 3: Correlated variations with Z of α^2 (solid circles) and $\sum_i u_i v_i$ (open circles) for $T_z = 0$ nuclei calculated within the HTDA approach.

The large values of the isospin-mixing parameter found particularly in the $T_z = 0$ doubly-magic nuclei can be explained as follows taking the example of ^{40}Ca . As can be seen in Table II, the Coulomb contribution to the isospin mixing in HTDA calculations can be considered as small. We can therefore make the approximation that the neutron and proton single-particle states of ^{40}Ca are virtually identical and use Eq. (15) to estimate α^2 . Moreover, the largely dominant contributions to the particle-hole excitation expansion of $|\Psi\rangle$ in Eqs. (5) and (6) come from one-pair excitations so that we can write α^2 approximately as

$$\alpha^2 \approx \frac{1}{2(T_0 + 1)} \left[(\chi_0^{(n)})^2 \sum_{j \neq 0} (\chi_j^{(p)})^2 \mathcal{R}(\Phi_0^{(n)}, \Phi_j^{(p)}) + (\chi_0^{(p)})^2 \sum_{i \neq 0} (\chi_i^{(n)})^2 \mathcal{R}(\Phi_0^{(p)}, \Phi_i^{(n)}) + \sum_{\substack{i \neq 0 \\ j \neq 0}} (\chi_i^{(n)})^2 (\chi_j^{(p)})^2 \mathcal{R}(\Phi_i^{(n)}, \Phi_j^{(p)}) \right], \quad (19)$$

where the relative excitation order of $|\Phi_i^{(n)}\rangle$ with respect to

$\Phi_j^{(p)}$ is simply given, here, by

$$\mathcal{R}(\Phi_i^{(n)}, \Phi_j^{(p)}) = \begin{cases} 0 & \text{if } i = 0, j = 0; \\ 2 & \text{if } i = 0, j \neq 0 \text{ or } i \neq 0, j = 0; \\ 4 & \text{otherwise.} \end{cases} \quad (20)$$

Since the states $|\Psi^{(q)}\rangle$ are normalized to unity, we have

$$\sum_{i \neq 0} (\chi_i^{(q)})^2 = 1 - (\chi_0^{(q)})^2, \quad (21)$$

and we finally obtain

$$\alpha^2 \approx \frac{1}{T_0 + 1} \left[2 - (\chi_0^{(n)})^2 - (\chi_0^{(p)})^2 \right]. \quad (22)$$

Since Eq. (22) overestimates the importance of one-pair excitations in $|\Psi\rangle$ through the estimates of Eq. (20) and given the very small contribution to $|\Psi\rangle$ coming from the particle-hole excitations other than one-pair excitations, we conclude that the value of α^2 calculated with Eq. (22) should lie between the values obtained in the full HTDA calculations without and with Coulomb interaction. In the case of ^{40}Ca , we find $(\chi_0^{(n)})^2 = 0.9804$ and $(\chi_0^{(p)})^2 = 0.9825$. This yields $\alpha^2 \approx 3.7\%$, which is slightly larger than the 3.5% obtained in the HTDA calculation without Coulomb interaction and smaller than the value of 4.2% from the full HTDA calculation, as expected.

Finally, it is interesting to note (see Table II) that the value of α^2 for a given nucleus obtained in a full HTDA calculation can be written, to a good approximation, as the sum of the ‘‘no Coulomb’’ HTDA result (including pairing correlations) and the ‘‘HF’’ result (no pairing, but including the full Coulomb field).

D. Discussion

In Fig. 4 we compare, for the above eight $N = Z$ nuclei, the α^2 values calculated in our HTDA model with the estimates obtained in the hydrodynamical model of Bohr, Damgård and Mottelson [4], and with the calculations by Hamamoto and Sagawa [10] in the Hartree-Fock-plus-RPA approach with the SIII Skyrme interaction. Each model predicts an increasing trend of α^2 with Z . The HTDA approach, as presently applied with $|T_z| = 1$ pairing correlations only, predicts a larger isospin mixing than the RPA calculations (which do not include pairing correlations).

It is important to recall that only $|T_z| = 1$ pairing correlations are considered here. We expect the values of α^2 obtained by including, in addition, pairing correlations in the $T_z = 0$ channel to be smaller than the present values. Indeed, in presence of proton-neutron correlations, the $|T_z| = 1$ pairing correlations, being effected by a smaller probability amplitude, would contribute less to the total HTDA wave function. Correlatively, they would be replaced essentially by configurations of the type $a_i^\dagger a_j |\Phi_0^{(n)}\rangle \otimes a_k^\dagger a_\ell |\Phi_0^{(p)}\rangle$ where the neutron and proton hole states $|j\rangle$ and $|\ell\rangle$ on the one hand, the neutron and proton particle states $|i\rangle$

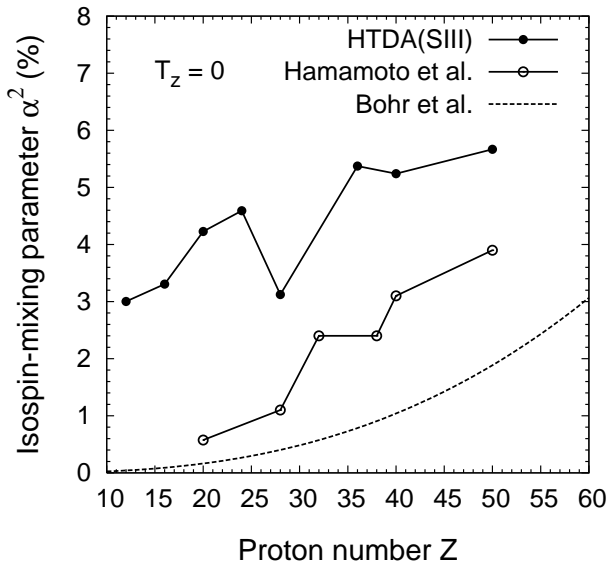


FIG. 4: Variation with Z of the isospin-mixing parameter α^2 of $T_z = 0$ nuclei calculated within the HTDA approach (solid circles), by Hamamoto *et al.* [10] in the RPA approach (open circles) and by Bohr *et al.* [4] in a hydrodynamical model (dashed line).

and $|k\rangle$ on the other hand, are similar. The relative excitation order between two such one-particle–one-hole neutron, one-particle–one-hole proton configurations would thus be on average smaller than that between two one-pair excitation neutron, one-pair excitation proton configurations which reaches about 4 from Eq. (20). However, the further addition of RPA correlations, which can be treated in the HTDA framework on the same footing as the pairing correlations, would compensate the effect of the $T_z = 0$ pairing correlations and the net result may be close to the present result.

IV. CONCLUSION

We have shown that the HTDA approach is a reliable model to address the isospin–mixing issue because such an approach can include the pairing correlations in a consistent way while conserving the particle-number, in contrast to Hartree–Fock–Bogoliubov and Hartree–Fock–BCS treatments.

From HTDA calculations, we have learned that the difference between the neutron and proton masses has a negligible impact on the expectation value of $\hat{\mathbf{T}}^2$ and that the effect of the Coulomb interaction is rather small as compared to the effect of the $|T_z| = 1$ correlations. Moreover the stronger isospin symmetry breaking is found in the $N = Z$ nuclei.

To obtain a more complete description, both neutron–proton pairing and RPA-type correlations need to be taken into account. Both of these can be included in the HTDA framework in a consistent way. It is expected that these two

types of correlations affect the present results with opposite signs. Such a study is currently under way.

ACKNOWLEDGMENTS

One of the authors (Ph. Q.) acknowledge the Theoretical Division at LANL for the excellent working conditions extended to him during numerous visits. This work has been supported by the U.S. Department of Energy under contract W-7405-ENG-36.

APPENDIX A. ISOSPIN OPERATOR $\hat{\mathbf{T}}^2$ AND ONE- AND TWO-BODY MATRIX ELEMENTS

The operator $\hat{\mathbf{T}}^2$ can be written as the sum of a one-body operator \hat{O}_1 and a two-body operator \hat{O}_2 acting in the Fock space

$$\hat{\mathbf{T}}^2 = \hat{O}_1 + \hat{O}_2, \quad (\text{A-1})$$

$$\hat{O}_1 = \sum_i \hat{\mathbf{t}}_i^2, \quad (\text{A-2})$$

$$\hat{O}_2 = \frac{1}{2} \sum_{i \neq j} 2(\hat{\mathbf{t}}_i \otimes \hat{\mathbf{t}}_j), \quad (\text{A-3})$$

where $\hat{\mathbf{t}}_i \otimes \hat{\mathbf{t}}_j = \hat{t}_x \otimes \hat{t}_x + \hat{t}_y \otimes \hat{t}_y + \hat{t}_z \otimes \hat{t}_z$. We define the one-body and two-body operators \hat{o}_1 and \hat{o}_2 acting in the one-particle space and the two-particle space, respectively, by

$$\hat{o}_1 = \hat{\mathbf{t}}^2, \quad (\text{A-4})$$

$$\hat{o}_2 = 2(\hat{\mathbf{t}} \otimes \hat{\mathbf{t}}) = 2(\hat{t}_x \otimes \hat{t}_x + \hat{t}_y \otimes \hat{t}_y + \hat{t}_z \otimes \hat{t}_z). \quad (\text{A-5})$$

Introducing the operators \hat{t}_+ and \hat{t}_- defined by

$$\hat{t}_+ = \hat{t}_x + i\hat{t}_y, \quad (\text{A-6})$$

$$\hat{t}_- = \hat{t}_x - i\hat{t}_y, \quad (\text{A-7})$$

we can rewrite \hat{o}_2 as

$$\hat{o}_2 = \hat{t}_+ \otimes \hat{t}_- + \hat{t}_- \otimes \hat{t}_+ + 2(\hat{t}_z \otimes \hat{t}_z). \quad (\text{A-8})$$

The Hartree–Fock basis is built up from the single-particle states generically noted $|i\rangle$. They describe either a neutron state or a proton state, so they are eigenstates of the isospin operators $\hat{\mathbf{t}}^2$ and \hat{t}_z

$$\hat{\mathbf{t}}^2|i\rangle = \frac{3}{4}|i\rangle \quad (\text{A-9})$$

$$\hat{t}_z|i\rangle = \tau_i|i\rangle = \begin{cases} \frac{1}{2}|i\rangle & \text{neutron} \\ -\frac{1}{2}|i\rangle & \text{proton.} \end{cases} \quad (\text{A-10})$$

In practice, we expand the single-particle states $|i\rangle$ on the cylindrical harmonic oscillator (HO) basis $\{|\alpha\rangle\}$ as follows

$$|i\rangle = \sum_{\alpha} C_{\alpha}^{(i)}|\alpha\rangle \otimes |t \tau_i\rangle, \quad (\text{A-11})$$

where α stands for the 4 quantum numbers n_z , n_\perp , Λ (eigenvalue of $\hat{\ell}_z$) and Σ (eigenvalue of \hat{s}_z), $t = 1/2$ and $\tau_i = \pm 1/2$ depending on the nature of the particle.

The action of the operators \hat{t}_- and \hat{t}_+ on the single-particle states $|i\rangle$ is given by

$$\hat{t}_- |i\rangle = \delta_{in} \sum_{\alpha} C_{\alpha}^{(i)} |\alpha\rangle \otimes |t\tau_i - 1\rangle, \quad (\text{A-12})$$

$$\hat{t}_+ |i\rangle = \delta_{ip} \sum_{\alpha} C_{\alpha}^{(i)} |\alpha\rangle \otimes |t\tau_i + 1\rangle. \quad (\text{A-13})$$

The matrix elements of \hat{t}_- and \hat{t}_+ in the Hartree-Fock basis thus write

$$\langle i|\hat{t}_-|k\rangle = \delta_{ip}\delta_{kn} \langle i|k\rangle_{\text{space-spin}}, \quad (\text{A-14})$$

$$\langle i|\hat{t}_+|k\rangle = \delta_{in}\delta_{kp} \langle i|k\rangle_{\text{space-spin}}. \quad (\text{A-15})$$

In the above equations and elsewhere in this paper, the subscript ‘‘space-spin’’ attached to an overlap of single-particle states means that the overlap is restricted to the space and spin variables only. This allows to consider such overlaps between two nucleonic states corresponding to different charges. Since the time reversal operator does not act on isospin, we have

$$\langle i|\hat{t}_{\pm}|\bar{k}\rangle = 0, \quad (\text{A-16})$$

where $|\bar{k}\rangle$ is the time-reversed conjugate state of $|k\rangle$, and

$$\langle \bar{i}|\hat{t}_{\pm}|\bar{k}\rangle = \langle i|\hat{t}_{\pm}|k\rangle. \quad (\text{A-17})$$

From Eq. (A-9) we easily get

$$\langle i|\hat{o}_1|j\rangle = \frac{3}{4} \delta_{ij} \quad (\text{A-18})$$

and using Eqs. (A-8), (A-14) and (A-15), we can write the two-body matrix element $\langle ij|\hat{o}_2|k\ell\rangle$ as

$$\begin{aligned} \langle ij|\hat{o}_2|k\ell\rangle &= 2\tau_i\tau_j\delta_{ik}\delta_{j\ell} + (\delta_{ip}\delta_{kn}\delta_{jn}\delta_{\ell p} + \delta_{in}\delta_{kp}\delta_{jp}\delta_{\ell n}) \times \\ &\langle i|k\rangle_{\text{space-spin}} \langle j|\ell\rangle_{\text{space-spin}}. \end{aligned} \quad (\text{A-19})$$

To close this appendix, we recall useful expressions for the expectation value of one-body and two-body operators in a Slater determinant $|\Phi_i\rangle$ and related matrix elements. For a one-body operator \hat{O}_1 we have

$$\langle \Phi_i|\hat{O}_1|\Phi_i\rangle = \sum_{k \in \Phi_i} \langle k|\hat{o}_1|k\rangle, \quad (\text{A-20})$$

$$\langle \Phi_i|\hat{O}_1 a_k^\dagger a_j |\Phi_i\rangle = \delta_j^h \delta_k^p \langle j|\hat{o}_1|k\rangle, \quad (\text{A-21})$$

where the sum $\sum_{k \in \Phi_i}$ runs over the occupied single-particle states $|k\rangle$ of the Slater determinant $|\Phi_i\rangle$. In Eq. (A-21) and below, δ_j^h (resp. δ_k^p) is equal to 1 if $|j\rangle$ (resp. $|k\rangle$) is a hole state (resp. particle state) with respect to $|\Phi_i\rangle$ and 0 otherwise. For two-body operators we have

$$\langle \Phi_i|\hat{O}_2|\Phi_i\rangle = \frac{1}{2} \sum_{j,k \in \Phi_i} \langle jk|\hat{o}_2|j\bar{k}\rangle, \quad (\text{A-22})$$

$$\langle \Phi_i|\hat{O}_2 a_\ell^\dagger a_k |\Phi_i\rangle = \delta_k^h \delta_\ell^p \sum_{j \in \Phi_i} \langle jk|\hat{o}_2|j\bar{\ell}\rangle, \quad (\text{A-23})$$

$$\langle \Phi_i|\hat{O}_2 a_{k_1}^\dagger a_{k_2}^\dagger a_{j_1} a_{j_2} |\Phi_i\rangle = \delta_{j_1}^h \delta_{j_2}^h \delta_{k_1}^p \delta_{k_2}^p \langle j_1 j_2|\hat{o}_2|\bar{k}_1 \bar{k}_2\rangle, \quad (\text{A-24})$$

where $|\bar{i}\bar{j}\rangle = |ij\rangle - |ji\rangle$.

APPENDIX B. COMPARISON OF TWO SLATER DETERMINANTS

Let us consider two Slater determinants $|\Phi_i\rangle$ and $|\Phi_j\rangle$ built from the same set of orthonormal single-particle basis states. They may therefore be thought of as n -particle– n -hole and n' -particle– n' -hole excitations on a reference Slater determinant which may be chosen as the Hartree-Fock ground state $|\Phi_0\rangle$

$$|\Phi_i\rangle = a_{\beta_1}^\dagger \cdots a_{\beta_n}^\dagger a_{b_1} \cdots a_{b_n} |\Phi_0\rangle, \quad (\text{B-1})$$

$$|\Phi_j\rangle = a_{\gamma_1}^\dagger \cdots a_{\gamma_{n'}}^\dagger a_{c_1} \cdots a_{c_{n'}} |\Phi_0\rangle, \quad (\text{B-2})$$

where $\beta_1 < \cdots < \beta_n$ and $\gamma_1 < \cdots < \gamma_{n'}$ are two sets of particle states (with respect to $|\Phi_0\rangle$) and $b_1 < \cdots < b_n$ and $c_1 < \cdots < c_{n'}$ are two sets of hole states. We can express $|\Phi_j\rangle$ as a function of $|\Phi_i\rangle$ as

$$|\Phi_j\rangle = a_{\gamma_1}^\dagger \cdots a_{\gamma_{n'}}^\dagger a_{c_1} \cdots a_{c_{n'}} a_{b_n}^\dagger \cdots a_{b_1}^\dagger a_{\beta_n} \cdots a_{\beta_1} |\Phi_i\rangle. \quad (\text{B-3})$$

We denote by \mathcal{H} the set of hole states in common between $\{b_1, \cdots, b_n\}$ and $\{c_1, \cdots, c_{n'}\}$

$$\mathcal{H} = \{c_{h'_i} = b_{h_i}, 1 \leq i \leq N_h\}, \quad (\text{B-4})$$

where N_h is the number of hole states in common. Similarly \mathcal{P} is the set of particle states in common between $\{\beta_1, \cdots, \beta_n\}$ and $\{\gamma_1, \cdots, \gamma_{n'}\}$

$$\mathcal{P} = \{\gamma_{p'_i} = \beta_{p_i}, 1 \leq i \leq N_p\}, \quad (\text{B-5})$$

where N_p is the number of hole states in common. Therefore it can be shown that

$$\begin{aligned} |\Phi_j\rangle &= \\ \varphi_{ij} &\left(\prod_{\substack{k=1 \\ \gamma_k \notin \mathcal{P}}}^{n'} a_{\gamma_k}^\dagger \right) \left(\prod_{\substack{k=n \\ b_k \notin \mathcal{H}}}^1 a_{b_k}^\dagger \right) \left(\prod_{\substack{k=1 \\ c_k \notin \mathcal{H}}}^{n'} a_{c_k} \right) \left(\prod_{\substack{k=n \\ \beta_k \notin \mathcal{P}}}^1 a_{\beta_k} \right) |\Phi_i\rangle, \end{aligned} \quad (\text{B-6})$$

where the associated relative phase is given by

$$\varphi_{ij} = (-1)^{n+n'+N_h + \sum_{k=1}^{N_h} (h_i - h'_i) + \sum_{k=1}^{N_p} (p_i - p'_i)}. \quad (\text{B-7})$$

Changing the order of the creation and/or annihilation operators in Eq. (B-6) would change the sign of φ_{ij} .

Finally the relative excitation order $\mathcal{R}(\Phi_i, \Phi_j)$ between the two Slater determinants $|\Phi_i\rangle$ and $|\Phi_j\rangle$, defined as the number of creation (or annihilation) operators in Eq. (B-6), is simply given by

$$\mathcal{R}(\Phi_i, \Phi_j) = n + n' - (N_h + N_p). \quad (\text{B-8})$$

APPENDIX C. NUCLEAR SHAPE AND SIZE QUANTITIES

Starting from the nuclear shape determined in a self-consistent way by the HTDA solution, we can extract a quadrupole deformation parameter β_2 by approximating the nuclear shape by the equivalent spheroid having the same root-mean-square mass radius r_m and mass quadrupole moment Q_{20} as the actual nucleus. The semi-axes c (along the symmetry axis) and a (in the perpendicular direction) are related to r_m and Q_{20} through

$$A r_m^2 = \int d^3\mathbf{r} \rho(\mathbf{r}) \mathbf{r}^2 = \frac{1}{5}(2a^2 + c^2), \quad (\text{C-1})$$

$$Q_{20} = 2 \int d^3\mathbf{r} \rho(\mathbf{r}) \mathbf{r}^2 P_2(\cos\theta) = \frac{2}{5} A (c^2 - a^2), \quad (\text{C-2})$$

where $A = N + Z$, $\rho(\mathbf{r})$ is the isoscalar nuclear density (sum of neutron and proton contributions) and P_2 is the Legendre polynomial of degree 2.

The β_2 parameter is then calculated for this equivalent spheroid by expanding the nuclear radius in polar coordinates according to the β_l -parametrization [18]

$$R(\theta) = \frac{a}{\sqrt{1 - \alpha \cos^2\theta}} \quad (\text{C-3})$$

$$= R_0 \left(1 + \sum_{l=1}^{\infty} \beta_l Y_l^0(\theta) \right), \quad (\text{C-4})$$

with

$$\alpha = 1 - \frac{a^2}{c^2}. \quad (\text{C-5})$$

This allows us to derive the analytical expression of β_2 for the equivalent spheroid as a function of α as

$$\beta_2 = \begin{cases} \sqrt{5\pi} \left[\frac{3}{2\alpha} \left(1 - \frac{\sqrt{\alpha(1-\alpha)}}{\text{Arcsin}\sqrt{\alpha}} \right) - 1 \right] & \alpha \in]0; 1[\\ 0 & \alpha = 0 \\ \sqrt{5\pi} \left[\frac{3}{2\alpha} \left(1 - \frac{\sqrt{-\alpha(1-\alpha)}}{\ln(\sqrt{-\alpha} + \sqrt{1-\alpha})} \right) - 1 \right] & \alpha < 0 \end{cases}. \quad (\text{C-6})$$

As for the mass hexadecapole moment Q_{40} , we calculate it using the following expression with usual notation

$$Q_{40} = \int d^3\mathbf{r} \rho(\mathbf{r}) r^4 Y_4^0(\theta). \quad (\text{C-7})$$

Finally, the charge radius r_c is calculated as in Refs. [19, 20] through

$$r_c^2 = \int d^3\mathbf{r} \int d^3\mathbf{s} f_p(\mathbf{r} - \mathbf{s}) \rho_p(\mathbf{r}) \mathbf{r}^2, \quad (\text{C-8})$$

where $\rho_p(\mathbf{r})$ is the proton density and $f_p(\mathbf{x})$ denotes the proton form factor. With a Gaussian form for the latter, $f_p(\mathbf{x}) = \exp(-\mathbf{x}^2/r_0^2)/(r_0\sqrt{\pi})$, we have

$$r_c^2 = r_p^2 + \frac{3}{2} r_0^2, \quad (\text{C-9})$$

with

$$r_p^2 = \int d^3\mathbf{r} \rho_p(\mathbf{r}) \mathbf{r}^2. \quad (\text{C-10})$$

In our calculations we choose to use the value $r_0 = 0.65$ fm ($\frac{3}{2}r_0^2 = 0.64$ fm²) from Ref. [20].

APPENDIX D. TECHNICAL ASPECTS OF THE CALCULATIONS

We illustrate in this appendix the importance of several technical aspects of the mean-field calculations that can have a substantial impact on the quality of the results for the isospin-mixing parameter α^2 .

First, the choice of the reference Slater determinant $|\Phi_0\rangle$ for HTDA calculations is very important. Figure 5 shows the variation of the isospin-mixing parameter α^2 calculated within the HTDA approach with the number of preliminary HFBCS iterations, in the case of ⁴⁸Cr. As an initial potential we choose the Woods–Saxon potential including a spin-orbit term with the same parameters for neutron and protons (hence without Coulomb interaction for the first iteration). From the decreasing and saturating trend

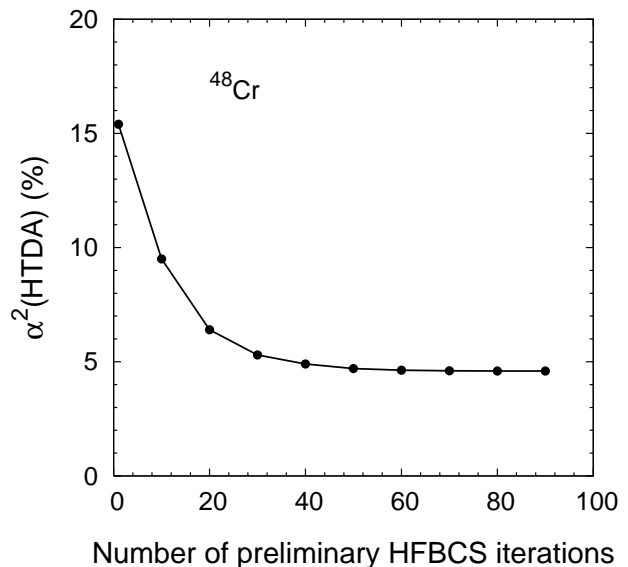


FIG. 5: Variation of the isospin-mixing parameter α^2 calculated within the HTDA approach with the number of preliminary HFBCS iterations, in the case of ⁴⁸Cr.

obtained here, we conclude that the consistency of the underlying mean-field from which $|\Phi_0\rangle$ is determined plays an important role. In other words a poor mean-field is a source of spurious isospin symmetry breaking.

The second aspect of importance is the convergence of α^2 with the number m of Slater determinants contributing to $|\Psi\rangle$ retained in the calculation of $\langle\Psi|\hat{T}^2|\Psi\rangle$. The Slater determinants $|\Phi_i^{(q)}\rangle$ entering the expansion (6) of $|\Psi^{(q)}\rangle$ are

arranged in decreasing order of $|\chi_i^{(q)}|$. The results are shown in Fig. 6, whereas in Fig. 7 we present the variation of the neutron and proton Slater determinant amplitudes $|\chi_m|$ with m .

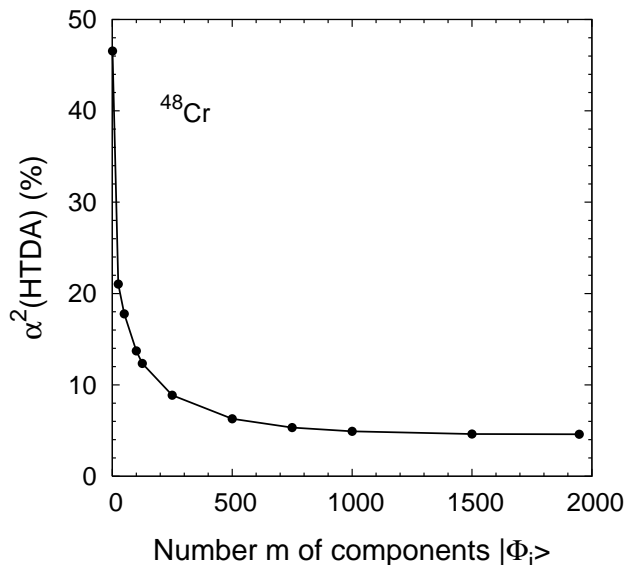


FIG. 6: Variation of α^2 with the number of Slater determinants $|\Phi_i\rangle$, from the expansion of the HTDA ground state $|\Psi\rangle$, that are used to calculate α^2 .

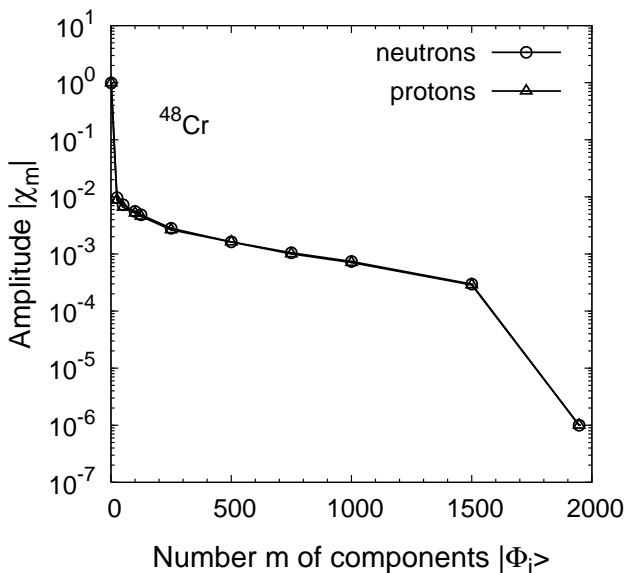


FIG. 7: Variation of the neutron (open circles) and proton (open triangles) Slater determinant amplitudes $|\chi_m|$ with the number m of Slater determinants retained from the expansion of $|\Psi\rangle$ for the calculation of α^2 . The first point is for $m = 1$, the dominant component in $|\Psi\rangle$.

Finally, we have checked for three nuclei that the values of the isospin-mixing parameter calculated in the HTDA approach is not sensitive to the procedure of optimization of the harmonic oscillator basis parameters b and q (with the notation of Ref. [17]), namely at the level of the preliminary HFBCS calculations or at the final stage of our HTDA approach. The optimized values of b and q obtained in each of the two schemes are reported in Table III together with the resulting values of α^2 for ^{24}Mg , ^{40}Ca and ^{80}Zr . We recall that the cylindrical harmonic oscillator basis used in all calculations contains 15 major shells, which corresponds to $N_0 = 14$ in the notation of Ref. [17].

TABLE III: Optimized values of b and q obtained in the two optimization schemes (at the level of the preliminary HFBCS calculations or at the final stage of the HTDA calculations) and resulting values of the isospin-mixing parameter α^2 calculated in the HTDA approach for ^{24}Mg , ^{40}Ca and ^{80}Zr .

Nucleus	HFBCS optimization			HTDA optimization		
	b	q	α^2 (%)	b	q	α^2 (%)
^{24}Mg	0.65	1.28	3.001	0.65	1.05	2.999
^{40}Ca	0.66	1.00	4.228	0.66	1.00	4.228
^{80}Zr	0.60	1.37	5.229	0.58	1.45	5.264

-
- [1] Å. Bohr and B. R. Mottelson, *Nuclear Structure*, Vol. 1 (Benjamin, New York, 1969), p. 36.
- [2] R. J. Blin-Stoyle, in *Isospin in Nuclear Physics* (Ed. Sir D. H. Wilkinson, North Holland, Amsterdam, 1969), Chapter 4, pp. 115-172.
- [3] J. C. Hardy and I. S. Towner, *Phys. Rev. C* **71**, 055501 (2005).
- [4] Å. Bohr, J. Damgård, and B. R. Mottelson, in *Nuclear structure* (Eds. A. Hossain, Harun-ar-Rashid and M. Islam, North Holland, Amsterdam, 1967), p. 1.
- [5] A. M. Lane and J. M. Soper, *Nucl. Phys.* **37**, 363 (1962).
- [6] M. A. Bentley, C. D. O'Leary, A. Poves, G. Martínez-Pinedo, D. E. Appelbe, R. A. Bark, D. M. Cullen, S. Ertürk, and A. Maj, *Phys. Lett.* **437B**, 243 (1998); erratum *Phys. Lett.* **451B**, 445 (1999).
- [7] A. P. Zuker, S. M. Lenzi, G. Martínez-Pinedo, and A. Poves, *Phys. Rev. Lett.* **89**, 142502 (2002).
- [8] W. E. Ormand, *Phys. Rev. Lett.* **82**, 1101 (1999).
- [9] P. Navrátil, B. R. Barrett, and W. E. Ormand, *Phys. Rev. C* **56**, 2542 (1997).
- [10] I. Hamamoto and H. Sagawa, *Phys. Rev. C* **48** R960 (1993).
- [11] H. Sagawa, N. Van Giai, and T. Suzuki, *Phys. Rev. C* **53**, 2163 (1996).
- [12] N. Pillet, P. Quentin, and J. Libert, *Nucl. Phys.* **A697**, 141 (2002).
- [13] N. Pillet, N. Sandulescu, N. Van Giai, and J.-F. Berger, *Phys. Rev. C* **71**, 044306 (2005).
- [14] K. Sieja, T. L. Ha, P. Quentin, and A. Baran, *Int. J. Mod. Phys.* **E16**, 289 (2007).
- [15] L. Bonneau, P. Quentin, and K. Sieja, submitted to *Phys. Rev. C*.
- [16] M. Beiner, H. Flocard, N. Van Giai, and P. Quentin, *Nucl. Phys.* **A238**, 29 (1975).
- [17] H. Flocard, P. Quentin, A. K. Kerman, and D. Vautherin, *Nucl. Phys.* **A203**, 433 (1973).
- [18] P. Möller, J. R. Nix, W. D. Myers, and W. J. Swiatecki, *At. Data and Nucl. Data Tables* **59**, 185 (1995).
- [19] J. W. Negele, *Phys. Rev. C* **1**, 1260 (1970).
- [20] D. Vautherin and D. M. Brink, *Phys. Rev. C* **5**, 626 (1972).